Translational Oncology 16 (2022) 101313

Contents lists available at ScienceDirect

Translational Oncology

journal homepage: www.elsevier.com/locate/tranon

Original Research

Co-targeting MCL-1 and ERK1/2 kinase induces mitochondrial apoptosis in rhabdomyosarcoma cells

Marius Winkler, Juliane Friedrich, Cathinka Boedicker, Nadezda Dolgikh *

Institute for Experimental Cancer Research in Pediatrics, Goethe-University Frankfurt, Komturstr. 3a, 60528 Frankfurt, Germany

ARTICLE INFO

Keywords:
RMS
Ulixertinib
S63845
ERK1/2 signaling
Apoptotic cell death

ABSTRACT

The RAS/MEK/ERK genetic axis is commonly altered in rhabdomyosarcoma (RMS), indicating high activity of downstream effector ERK1/2 kinase. Previously, we have demonstrated that inhibition of the RAS/MEK/ERK signaling pathway in RMS is insufficient to induce cell death due to residual pro-survival MCL-1 activity. Here, we show that the combination of ERK1/2 inhibitor Ulixertinib and MCL-1 inhibitor S63845 is highly synergistic and induces apoptotic cell death in RMS *in vitro* and *in vivo*. Importantly, Ulixertinib/S63845 co-treatment suppresses long-term survival of RMS cells, induces rapid caspase activation and caspase-dependent apoptosis. Mechanistically, Ulixertinib-mediated upregulation of BIM and BMF in combination with MCL-1 inhibition by S63845 shifts the balance of BCL-2 proteins towards a pro-apoptotic state resulting in apoptosis induction. A genetic silencing approach reveals that BIM, BMF, BAK and BAX are all required for Ulixertinib/S63845-induced apoptosis. Overexpression of BCL-2 rescues cell death triggered by Ulixertinib/S63845 co-treatment, confirming that combined inhibition of ERK1/2 and MCL-1 effectively induces cell death of RMS cells via the intrinsic mitochondrial apoptotic pathway. Thus, this study is the first to demonstrate the cytotoxic potency of co-inhibition of ERK1/2 and MCL-1 for RMS treatment.

Introduction

Rhabdomyosarcoma (RMS) is an aggressive pediatric mesenchymal cancer characterized by a skeletal muscle phenotype. In terms of molecular characteristics, RMS can be classified as either PAX3/7-FOXO1 fusion-positive (FP) or fusion-negative (FN) tumors that correlate with histology, clinical outcome and prognosis of alveolar or embryonal RMS, respectively [1]. Currently, the standard multimodal treatment for RMS patients includes chemotherapeutic drugs, radiation and surgery [2]. However, this treatment regimen has severe side effects and limited efficacy as evident by the survival rates of less than 30% for patients with FP-RMS or metastatic RMS [3], highlighting the necessity of new targeted therapeutic options for RMS patients.

The RAS/MEK/ERK pathway has been well studied and its therapeutic potential has drawn immense attention in the treatment of cancer [4], since elements of this signaling pathway, including receptor tyrosine kinases (RTKs), regulators of RAS, RAS itself, BRAF and MEK1/2 are frequently mutated, leading to abnormal activation of ERK1/2 signaling that supports oncogenic growth, survival and apoptosis avoidance [5]. Aberrant RAS/MEK/ERK signaling is highly activated in RMS regardless of the fusion status [2,6], making the pathway an attractive target for therapeutic options. Indeed, the most common genetic aberration of FN-RMS are mutations in NRAS, KRAS, or HRAS which results in elevated ERK1/2 signaling in RMS cells. Interestingly, despite a different genetic background, FP-RMS are also associated with disrupted RTK/RAS/MEK/ERK signaling which is due either to their PAX gene rearrangement or to an increase in mutations of genes downstream of PAX3/7-FOXO1 fusion protein [6]. Beside, the pathology of FP-RMS often involves activation of growth factor receptor pathways (*e.g.* IGF and FGF) that activate downstream ERK1/2 signaling [7].

Abbreviations: (CAM), chicken chorioallantoic membrane; (CHX), cycloheximide; (CI), combination index; (DUSP6), dual specificity phosphatase 6; (EV), empty vector; (ERK), extracellular signal-regulated kinase; (FCS), fetal calf serum; (FGF), fibroblast growth factor; (FOXO1), forkhead box protein O1; (IGF), insulin-like growth factor; (MULE), MCL-1 ubiquitin ligase E3; (MEK), mitogen-activated protein kinase; (zVAD.fmk), N-benzyloxycarbonyl-Val-Ala-Asp(O-Me) fluoromethyl ketone; (Nec-1s), necrostatin-1s; (RSK), p90 ribosomal s6 kinase; (PAX), paired box; (FN), PAX3/7-FOXO1 fusion-negative; (FP), PAX3/7-FOXO1 fusion-positive; (PBMCs), peripheral blood mononuclear cells; (PARP), poly(ADP-ribose) polymerase; (PI), propidium iodide; (RIP1), receptor-interacting protein 1; (RTK), receptor tyrosine kinase; (RMS), rhabdomyosarcoma.

* Corresponding author.
E-mail address: n.dolgikh@kinderkrebsstiftung-frankfurt.de (N. Dolgikh).

https://doi.org/10.1016/j.tranon.2021.101313
Received 3 December 2021; Accepted 6 December 2021

Cancers with aberrant RAS/MEK/ERK signaling are currently treated with MEK1/2 and/or BRAF inhibitors [8]. However, the efficiency of this targeted therapy is limited due to acquired resistance which arises via reactivation of ERK1/2 kinase [9,10]. In light of acquired resistance towards MEK1/2 and BRAF inhibitors, direct inhibition of ERK1/2 kinase has attracted significant attention [11]. Ulixertinib (BVD-523, VRT752271), an orally available selective ERK1/2 inhibitor, recently entered clinical studies for the treatment of advanced solid tumors, pancreatic cancers, acute myeloid leukemia, and non-Hodgkin lymphomas [12,13]. Preclinical studies have shown that Ulixertinib proved to be more effective than MEK1/2 inhibitors for KRAS-mutated cells [14].

The intrinsic apoptosis pathway, also known as the mitochondrial pathway, largely contributes to the efficacy of targeted cancer therapies [15]. The intrinsic apoptotic pathway is orchestrated by BCL-2 family proteins, which are frequently dysregulated in cancers [16]. The BCL-2 family consists of anti-apoptotic proteins (*e.g.* MCL-1, BCL-2, BCL-X_L, BCL-W), pro-apoptotic BH3-only proteins (*e.g.* BIM, BMF, NOXA) and the pro-apoptotic multidomain effector proteins BAK and BAX. Under non-stress conditions, anti-apoptotic BCL-2 proteins bind and sequester BH3-only proteins, thereby preventing them from interacting with the executor proteins BAK and BAX. Upon apoptotic stimuli, specific BH3-only proteins are upregulated and activated, allowing BAK and BAX to undergo oligomerization. This results in outer mitochondrial membrane permeabilization and the release of mitochondrial pro-apoptotic proteins in the cytosol that subsequently promote apoptosome formation and activation of caspases leading to apoptosis [17].

In recent years, selective inhibitors of pro-survival BCL-2 proteins, called BH3 mimetics, have been developed that sensitize cancer cells towards mitochondrial apoptosis, especially in the context of insufficient apoptosis induction by targeted therapy [18]. While BH3 mimetics targeting BCL-2 and BCL-X_L have proved to be effective in preclinical and clinical studies, insufficient progress has been made in developing selective MCL-1 inhibitors. Recently, a highly potent MCL-1 inhibitor S63845 has been described to increase the efficacy of oncogenic kinase-targeted therapy [19].

We have previously reported that, despite increased expression of pro-apoptotic BIM and BMF proteins upon RAS/MEK/ERK signaling inhibition, the residual activity of the anti-apoptotic protein MCL-1 impedes cell death in RMS [20]. Moreover, MCL-1 overexpression is frequently observed in RMS samples [21] and is associated with resistance to RAS/MEK/ERK inhibition in different cancers [22]. Therefore, in the present study, we aim to explore the therapeutic potential of combined MCL-1 and ERK1/2 signaling inhibition in RMS.

Materials and methods

Cell culture and chemicals

RD, RMS13, TE381.T, MRC5, and C2C12 cell lines were obtained from the American Type Culture Collection (Manassas, Virginia, USA). RH30, RH18, and RH41 cell lines were obtained from the Deutsche Sammlung von Mikroorganismen und Zellkulturen GmbH. All cell lines were authenticated by short tandem repeats (STR) profiling and regularly tested for mycoplasma contaminations. Cells were grown in RPMI 1640 GlutaMAX-l medium or Dulbecco's Modified Eagles Medium (DMEM) GlutaMAX-l medium and supplemented with 10% fetal calf serum (FCS), 1 mM sodium pyruvate and 100 U/mL penicillin/streptomycin (all from Life Technologies, Eggenstein, Germany). RH18 and RH41 cells were supplemented with 20% FCS. Peripheral blood mononuclear cells (PBMCs) were isolated from the blood of healthy donors by the Deutsches Rotes Kreuz (Blutspendedienst, Frankfurt, Germany). All cells were cultured at 37 °C, 5% CO2 in a humidified incubator. Ulixertinib and SCH772984 were purchased from Selleck Chemicals (Houston, TX, USA), S63845 from Apexbio (Houston, TX, USA), Necrostatin-1s (Nec-1s) from Calbiochem (Merck, Darmstadt, Germany), N-Benzyloxycarbonyl-Val-Ala-Asp(O-Me) fluoromethyl ketone (zVAD.fmk) from Bachem (Heidelberg, Germany) and human recombinant TNFα from PeproTech (Hamburg, Germany). Smac mimetic BV6, dual cIAP and XIAP inhibitor, was kindly provided by Genentech. All other chemicals were purchased from Sigma-Aldrich (Taufkirchen, Germany) or Carl Roth (Karlsruhe, Germany), unless otherwise indicated.

Determination of cell death, number of viable cells, cell density and colony formation

Cell death was assessed by propidium iodide (PI) uptake of cells co-stained with a PI/Hoechst 33342 solution and measured and analyzed using an ImageXpress® Micro XLS Widefield High-Content Analysis System and MetaXpress® Software according to the manufacturer's instructions (Molecular Devices, Sunnyvale, CA, USA). Alternatively, cell death was assessed by measuring DNA fragmentation (sub-G1 fraction) of PI-stained nuclei by flow cytometry (FACS Canto II, BD Biosciences, Heidelberg, Germany) as described previously [23]. Apoptotic cell death was assessed by co-staining cells with Annexin V-FITC and PI and analyzed by flow cytometry.

The number of viable cells was determined based on the cells' metabolic activity using the MTT [3-(4,5-dimethylthiazol-2-yl)-2,5-diphenyltetrazolium bromide] assay according to the manufacturer's instructions (Roche Diagnostics, Mannheim, Germany). Cell density assay reflects detachment of adherent cells during cell death and was assessed by crystal violet staining. Treated cells were stained with crystal violet solution (0.5% crystal violet, 30% ethanol, 3% formaldehyde), air-dried and resuspended in 100 µl 1% SDS/well and absorbance measured with a Tecan Infinite M200 plate reader (Tecan, Mannedorf, Switzerland). For colony formation assay, cells were seeded in a six-well plate (200 cells for RMS13 and 600 cells for RH41) after pre-treatment with Ulixertinib and/or S63845 for 24 h. Cells were cultured for 12–14 days and then stained with crystal violet staining solution. Stained colonies were counted and the percentage of surviving colonies relative to untreated control was calculated.

Caspase activation assay

Cells were seeded at a density of 30,000 cells/cm^2 in 96-well plates and allowed to attach and grow overnight. The next day, cells were treated with Ulixertinib and/or S63845 and CellEvent Caspase-3/7 Green Detection Reagent according to the manufacturer's instructions (ThermoFisher Scientific). Fluorescence-based microscopic analysis of caspase-3/7 activity was performed using ImageXpress Micro XLS system (Molecular Devices). Imaged cells were analyzed with MetaXpress software using the Cell Scoring module that identifies Hoechst-33342-stained nuclei for a total cell count and classifies caspase-3/7-positive nuclei as apoptotic.

Western blot analysis and immunoprecipitation

Western blot analysis was performed as described previously [23], using the following antibodies: rabbit anti-BAX (1:1000, Millipore, ABC11), rabbit anti-BAK (1:1000, Millipore, 06–536), mouse anti-BCL-2 (1:1000, BD Biosciences, 610539), rabbit anti-BCL-X_L (1:1000, Cell Signaling, 2762S), rabbit anti-BCL-W (1:1000, Cell Signaling, 2724S), rabbit anti-pERK (Thr202/Tyr204) (1:1000, Cell Signaling, 9101S), rabbit anti-PUMA (1:1000, Cell Signaling, 4976S), rabbit anti-BIM (1:1000, Cell Signaling, 2819S), rabbit anti-p90 RSK (Ser380) (1:1000, Cell Signaling, 11989S), rabbit anti-RSK1 (1:1000, Cell Signaling, 8408S), mouse anti-PARP cleaved (1:1000, Cell Signaling, 9546S), rabbit anti-caspase-3 (1:1000, Cell Signaling, 9662S), rabbit anti-caspase-9 (1:1000, Cell Signaling, 9502S) rabbit anti-ERK (1:10000, Sigma, M5670), mouse anti-β-Actin (1:10000, Sigma, A5441), mouse anti-Vinculin (1:10000, Sigma, V9131), mouse

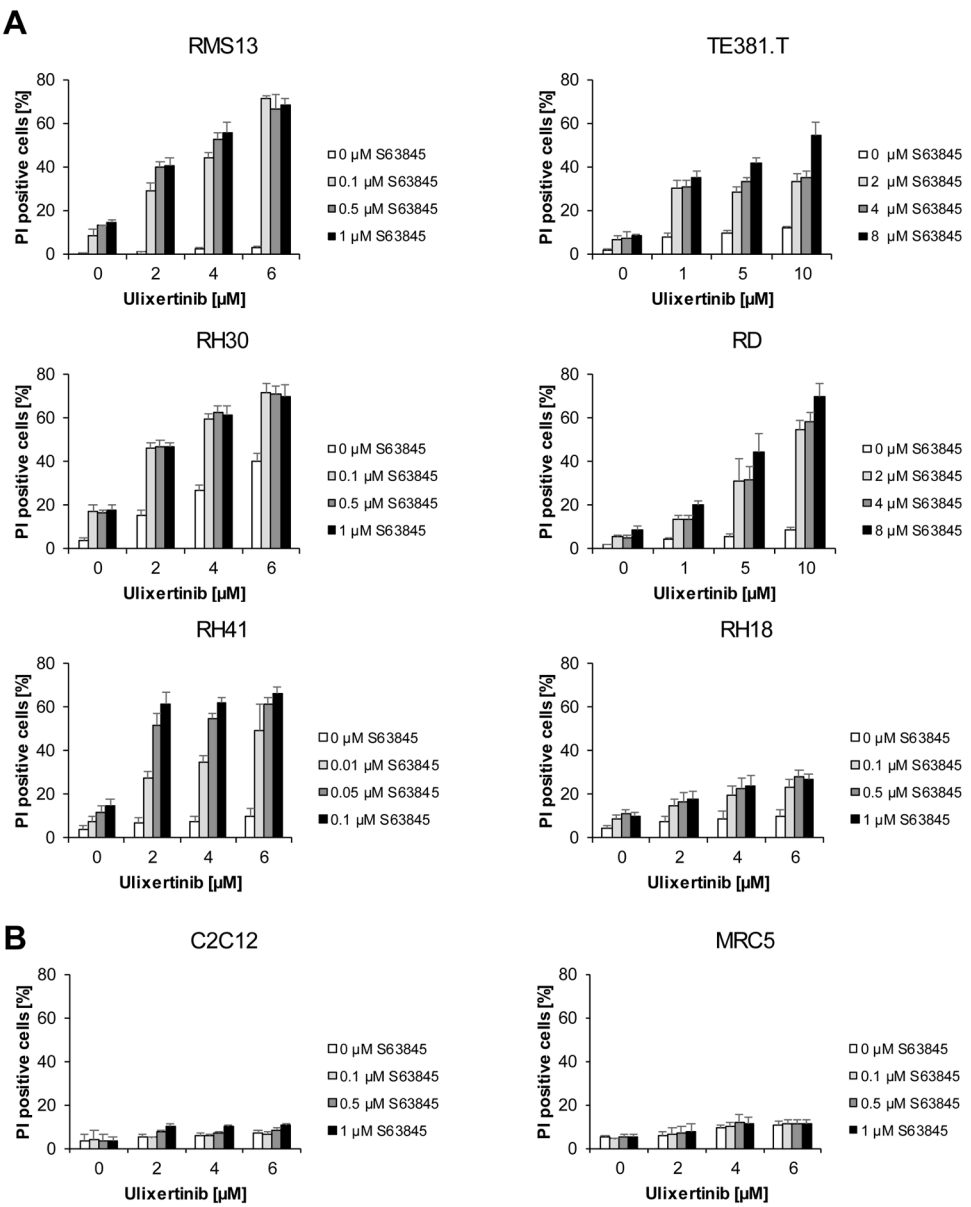

Fig. 1. Co-inhibition of ERK1/2 and MCL-1 induces cell death in RMS cells
Malignant RMS13, RH30, RH41, TE381.T, RD and RH18 cells (A) and non-malignant C2C12 and MRC5 cells (B) were treated with indicated concentrations of Ulixertinib and/or S63845 for 72 h and cell death was measured by fluorescent microscopy analysis of PI uptake using Hoechst 33342 and PI co-staining. Mean and SD (error bars) of three independent experiments performed in triplicates are shown.

anti-MKP-3 (DUSP6) (1:1000, Santa Cruz Biotechnology, sc-377070), rat anti-BMF (1:500, ENZO, ALX-804-343-C100), rabbit anti-MCL-1 (1:1000, ENZO, ADI-AAP-240-F), mouse anti-NOXA (1:1000, ENZO, ALX-804-408), mouse anti-GAPDH (1:5000, HyTest, 5G4cc(-6C5cc)). Membranes were incubated with primary antibody overnight at 4 °C with agitation followed by washing and one hour incubation at room temperature with secondary antibody: goat anti-mouse IgG (1:5000, Abcam, ab6789), goat anti-rat IgG (1:5000, Abcam, ab97057), and goat anti-rabbit IgG (1:5000, Abcam, ab6721) conjugated to horseradish peroxidase. Enhanced chemiluminescence (Amersham Bioscience, Freiburg, Germany) was used for detection. Immunoprecipitation of MCL-1 was performed as previously described [24]. The precipitate, input and flow through were analyzed for expression of BMF, BIM, and MCL-1 by Western blotting.

RNA interference and BCL-2 overexpression

Knockdowns were achieved by reverse transfection using Silencer®Select siRNA, OptiMEM Medium, and Lipofectamine RNAiMAX reagent according to the manufacturer's instructions (Life Technologies, Carlsbad, Germany). Non-silencing siRNA (4390843) or two or three distinct siRNA sequences were used to ensure on-target effects: siRNA for BIM (s195011, s195012, s223065); siRNA for BMF (s40385, s40386, and s40387); siRNA for MCL-1 (s8583 and s8585); siRNA for BAK (s1880 and s1881); siRNA for BAX (s1889 and s1890).

For BCL-2 overexpression, RMS cells were transfected with murine stem cell virus (pMSCV, Clontech, USA) containing murine BCL-2 or empty vector (EV), using calcium phosphate transfection followed by selection with Blasticidin as described previously [25].

Chicken chorioallantoic membrane (CAM) assay

RMS13 cells (2000,000 cells per egg) were mixed 1:1 with matrigel and implanted into the CAM of fertilized chicken eggs and allowed to form tumors. RMS13-derived tumors were treated with Ulixertinib and S63845 alone or in combination for two consecutive days. One day after the last treatment, tumors were fixed in 4% paraformaldehyde, and 3 µm thick paraffin sections were cut. The sections were subjected to immunohistochemical assessment using hematoxylin/eosin and cleaved caspase-3 staining (rabbit polyclonal antibody against cleaved caspase-3

Table 1
Synergistic cell death induction upon Ulixertinib/S63845. Bliss synergy scores were calculated using SynergyFinder tool as described in Materials and Methods for data shown in Fig. 1. Where Bliss synergy score <-10 is antagonism, from -10 to 10 is additivity, >10 is synergism. PAX3/7-FOXO1 fusion-negative (FN), PAX3/7-FOXO1 fusion-positive (FP).

Cell line	Bliss Synergy Score
RMS13 (FP, RAS wild-type)	42.645
RH41 (FP, RAS wild-type)	40.91
RH30 (FP, RAS wild-type)	34.257
RD (FN, NRAS mutation)	28.196
TE381.T (FN, NRAS mutation)	25.039
RH18 (FN, RAS wild-type)	10.603

(Asp175) (1:500, Cell Signaling, 9661S)). The images of the tumor sections were digitally captured, and cleaved caspase-3-positive area in relation to the entire tumor area was analysed independently by two investigators with Fiji, an image processing package in ImageJ (Version 1.8.0_172).

Statistical analysis and synergy calculation

For statistical significance, a one-way ANOVA followed by Dunnett's multiple comparisons test was performed using GraphPad Prism version 7.00 for Windows, GraphPad Software (La Jolla California USA). Drug interaction was analyzed by assessing Bliss synergy scores using online-tool SynergyFinder applying Bliss independence method as a reference model [26], where positive values (>10) indicate synergism, near zero (from -10 to 10) – additivity, negative values (<-10) – antagonism. Additionally, synergy of the drug interactions was assessed by calculation of combination index (CI) using CalcuSyn software (Biosoft) based on the methods described by Chou [27], where CI <0.9 indicates synergism, CI = 0.9–1.1 - additivity, and CI > 1.1 - antagonism.

Data availability

Primary data are available on request from the authors.

Results

Co-inhibition of ERK1/2 and MCL-1 induces cell death in RMS cells

First, we explored whether therapeutic strategies combining MCL-1 inhibitor with ERK1/2 signaling inhibition could be effective in RMS treatment. Therefore, we treated cells with Ulixertinib alone or in combination with MCL-1 inhibitor S63845 in a number of FP-RMS (RMS13, RH30, RH41) and FN-RMS cells (TE381.T, RD, RH18). In both, FP-RMS and FN-RMS, Ulixertinib/S63845 co-treatment induced cell death as measured by PI uptake (Fig. 1A). Bliss score calculation revealed that the combination of Ulixertinib/S63845 is highly synergistic in all cell lines tested, independently of PAX3/7-FOXO1 fusion or RAS mutational status (Table 1). Synergistic drug interaction of Ulixertinib/S63845 in RMS cells was also confirmed by calculation of CI (CI < 0.4) (Suppl. Table 1).

To confirm the specific mechanism of ERK1/2 inhibition, we treated RMS cells with SCH772984, a different ERK1/2 inhibitor, alone or in combination with S63845. Again, strong synergy was observed between MCL-1 inhibitor S63845 and the ERK1/2 inhibitor SCH772984 (Suppl. Fig. 1A, Suppl. Table 2). These results suggested that combining ERK1/2 inhibitors with MCL-1 inhibitor may be a promising combination

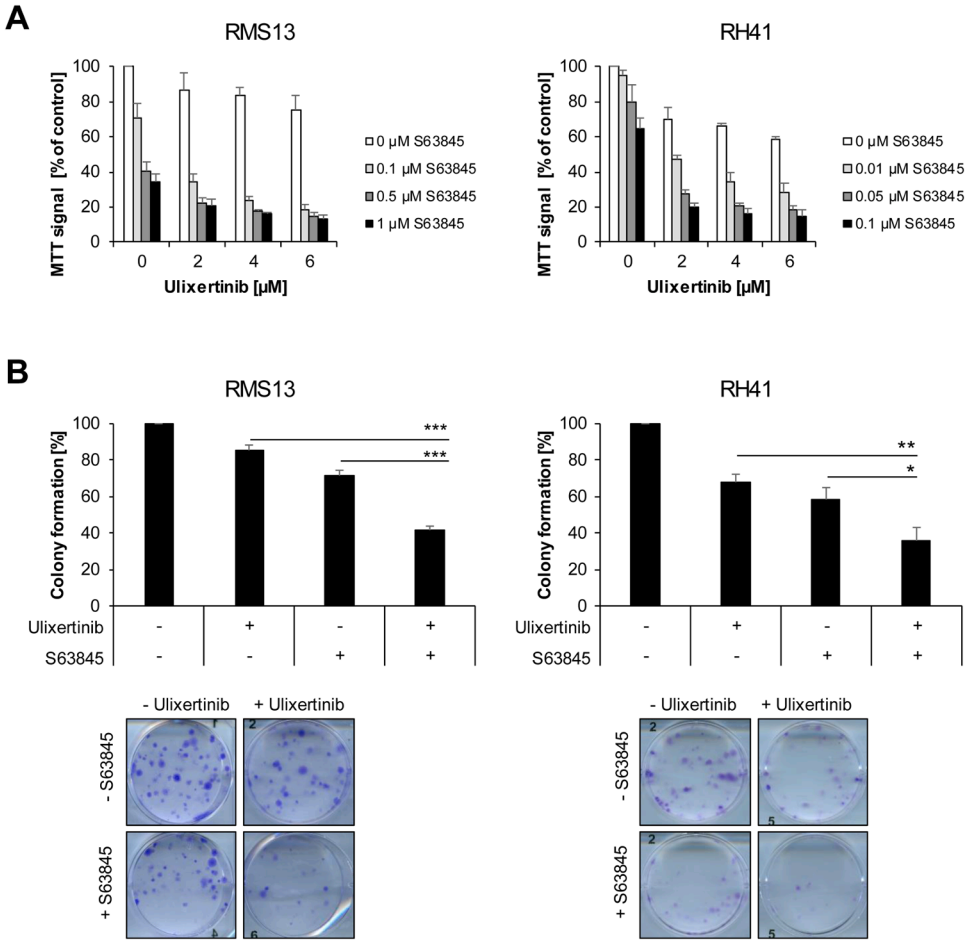

Fig. 2. Ulixertinib and S63845 cooperate to reduce cell viability and clonogenic growth
RMS13 and RH41 cells were treated for 72 h with indicated concentrations of Ulixertinib and/or S63845 and cell viability was measured using MTT assay (A). RMS13 and RH41 cells were treated with 6 µM Ulixertinib and 1 µM S63845 (RMS13) and 2 µM Ulixertinib and 0.1 µM S63845 (RH41) for 24 h and long-term clonogenic survival was assessed by colony formation assay. The number of surviving colonies is represented as a percentage of control. Representative images of one of three independent experiments are shown (B). Mean and SD (error bars) of three independent experiments performed in triplicates are shown, *, $P < 0.05$; **, $P < 0.01$; ***, $P < 0.001$.

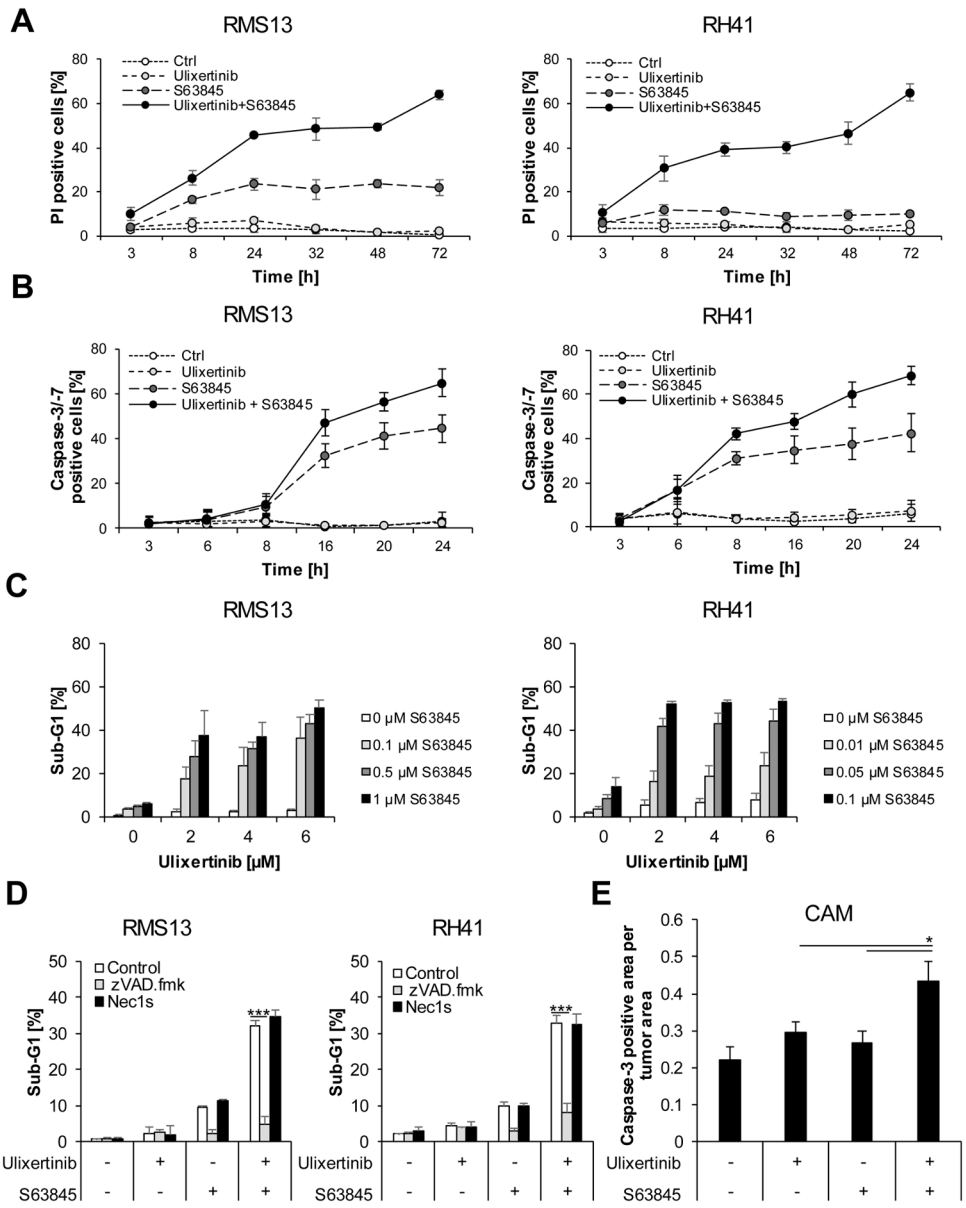

Fig. 3. Ulixertinib cooperates with S63845 to induce caspase-dependent cell death *in vitro* and in *vivo*

RMS13 and RH41 cells were treated with 6 µM Ulixertinib and/or 1 µM S63845 (RMS13) and 2 µM Ulixertinib and/or 0.1 µM S63845 (RH41) for indicated time points. Cell death kinetics were measured by fluorescent microscopy analysis of PI uptake using Hoechst 33342 and PI co-staining (A) or analysis of caspase-3/7 activity (B). RMS13 and RH41 cells were treated with indicated concentrations of Ulixertinib and/or S63845 for 72 h and cell death was measured by analysis of DNA fragmentation (Sub-G1 fraction) of PI-stained nuclei. Mean and SD (error bars) of three independent experiments performed in triplicates are shown (C). RMS13 and RH41 cells were pre-treated for 1 h with 50 µM zVAD.fmk or 10 µM Nec-1s before addition of 6 µM Ulixertinib and/or 1 µM S63845 (RMS13) and 2 µM Ulixertinib and/or 0.1 µM S63845 (RH41) and cell death was measured by analysis of DNA fragmentation (Sub-G1 fraction) of PI-stained nuclei after 48 h (D). Mean and SD (error bars) of three independent experiments performed in triplicates are shown, ***, $P < 0.001$. RMS13 cells were implanted on the CAM of fertilized chicken eggs and allowed to form tumors. RMS13-derived tumors were treated with 2 µM Ulixertinib and/or 0.1 µM S63845 over the next two days. The third day, tumors were resected and tumor sections were stained with an antibody that recognizes cleaved caspase-3. The area of cleaved caspase-3-positive cells in relation to the entire tumor area was quantified (E). Mean and SEM (error bars) of at least 12 eggs per group are shown, *, $P < 0.05$.

strategy for both FP- and FN-RMS.

Optimal combinational therapy should affect cancer cells and spare normal healthy cells, thereby increasing the therapeutic window over single-agent treatment. To test the effect of Ulixertinib/S63845 combination on normal cells, we treated C2C12 cells, derived from murine non-malignant myoblasts, and MRC5 cells, derived from human non-malignant lung fibroblasts. We showed that Ulixertinib and S63845 did not cooperate to induce cell death in these cells at similar concentrations that were highly synergistic in RMS cells (Fig. 1B). Additionally, Ulixertinib and S63845 alone or in combination did not trigger cell death in normal blood cells (*i.e.* PBMCs), confirming the absence of toxicity in non-malignant cells (Suppl. Fig. 1B).

Taken together, we showed that combined therapy by ERK1/2 and MCL-1 inhibition synergistically induced cell death in RMS cells while sparing healthy non-malignant cells, pointing to some tumor selectivity of this combination.

Ulixertinib and S63845 cooperate to reduce cell viability and clonogenic growth in RMS cells

Next, we analyzed the synergistic effect of Ulixertinib and S63845 in selected cell lines by examining cell survival upon treatment with both inhibitors. RMS13 and RH41 cell lines were chosen for further investigation based on highest Bliss synergy score (Table 1). In line with the results observed in cell death assays, the combination of Ulixertinib and S63845 significantly reduced survival of RMS13 and RH41 cells as measured by MTT assay (Fig. 2A). Moreover, we used a colony formation assay to assess long-term survival upon treatment. Combining Ulixertinib with S63845 also inhibited clonogenic survival of RMS cells (Fig. 2B). Therefore, co-inhibition of MCL-1 and ERK1/2 reduced cell viability and suppressed long-term clonogenic survival.

Ulixertinib cooperates with S63845 to induce caspase-dependent cell death

To investigate the mechanisms underlying this synergy between ERK1/2 inhibition and MCL-1 inhibition, we monitored the kinetics of the apoptotic response to Ulixertinib/S63845 co-treatment. Addition of

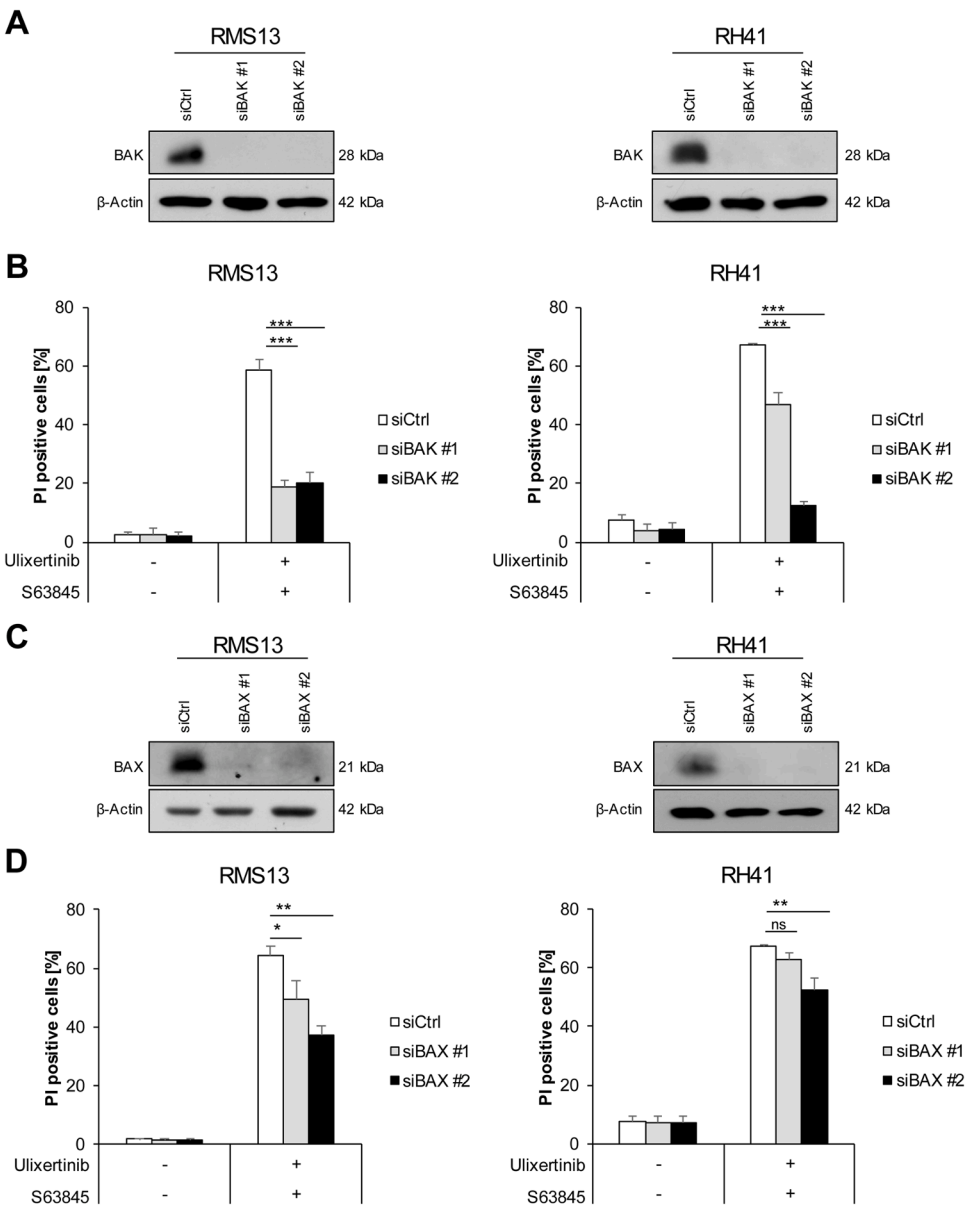

Fig. 4. BAK/BAX are required for Ulixertinib/S63845-induced apoptosis

RMS13 and RH41 cells were transiently transfected with non-silencing siRNA (siCtrl) or two distinct siRNA sequences targeting BAK (siBAK #1, siBAK #2) or BAX (siBAX #1, siBAX #2) and treated with 6 μM Ulixertinib and/or 1 μM S63845 (RMS13) and 2 μM Ulixertinib and/or 0.1 μM S63845 (RH41). Expression of BAK and BAX was assessed by Western blotting after 48 h. β-actin was used as a loading control. A representative blot of two independent experiments is shown (A, C). Cell death was measured after 72 h by fluorescent microscopy analysis of PI uptake using Hoechst 33342 and PI co-staining (B, D). Mean and SD (error bars) of three independent experiments performed in triplicates are shown, *, $P < 0.05$; **, $P < 0.01$; ***, $P < .001$, ns, not significant.

Ulixertinib to S63845 resulted in time-dependent increase in PI-positive cells (Fig. 3A). Accumulation of PI-positive cells was accompanied by caspase activation (Fig. 3B). This rapid induction of apoptosis was even more apparent at the level of caspase-3/7 activation, suggesting that the combination initiates the apoptotic machinery as early as 6–8 h after treatment.

Additionally, we analyzed cell detachment during Ulixertinib/S63845-induced apoptosis as evaluated by cell density using crystal violet assay. The combination treatment initiated a detachment of cells after 8 h of incubation with drugs (Suppl. Fig. 2A), indicating an early start of apoptotic processes.

Next, we verified the synergistic effect of Ulixertinib and S63845 by examining DNA fragmentation as a known marker of apoptotic cell death. The combination of Ulixertinib and S63845 was more potent to stimulate DNA fragmentation in RMS13 and RH41 cells as compared to Ulixertinib or S63845 single treatments, indicating synergistic apoptosis induction (Fig. 3C). To confirm apoptotic cell death induction upon the Ulixertinib/S63845 combination we used additional methods. Co-treatment with Ulixertinib and S63845 increased the percentage of late and early apoptotic cells as detected by Annexin V/PI co-staining (Suppl. Fig. 2B). Additionally, cleavage of Poly(ADP-ribose) polymerase (PARP), caspase-3, and -9 were observed upon the combinational treatment (Suppl. Fig. 2C).

To further explore whether caspases are required for Ulixertinib/S63845-induced apoptosis we applied the pan-caspase inhibitor zVAD.fmk. We discovered that the presence of zVAD.fmk almost completely rescued cells from cell death upon Ulixertinib/S63845 combination treatment (Fig. 3D). Additionally, we used Nec-1s, a Receptor-interacting protein (RIP)1 kinase inhibitor, to examine whether necroptosis is triggered upon the combination. A positive control for Nec-1s is shown in Suppl. Fig. 2D. Nec-1s failed to protect cells from cell death induction upon Ulixertinib/S63845 co-treatment (Fig. 3D). To investigate further antitumor effects of Ulixertinib/S63845 co-treatment *in vivo*, we applied the CAM assay, an established experimental model for anticancer drug validation *in vivo* [25,28]. RMS13 cells were implanted on the CAM of fertilized chicken eggs to form tumors and after treatment with Ulixertinib and/or S63845 cleaved caspase-3 positive cells were analyzed by immunohistochemical staining. Notably, Ulixertinib/S63845 co-treatment proved to be significantly more effective *in vivo* to trigger caspase-3 activation as a marker of apoptosis in RMS13

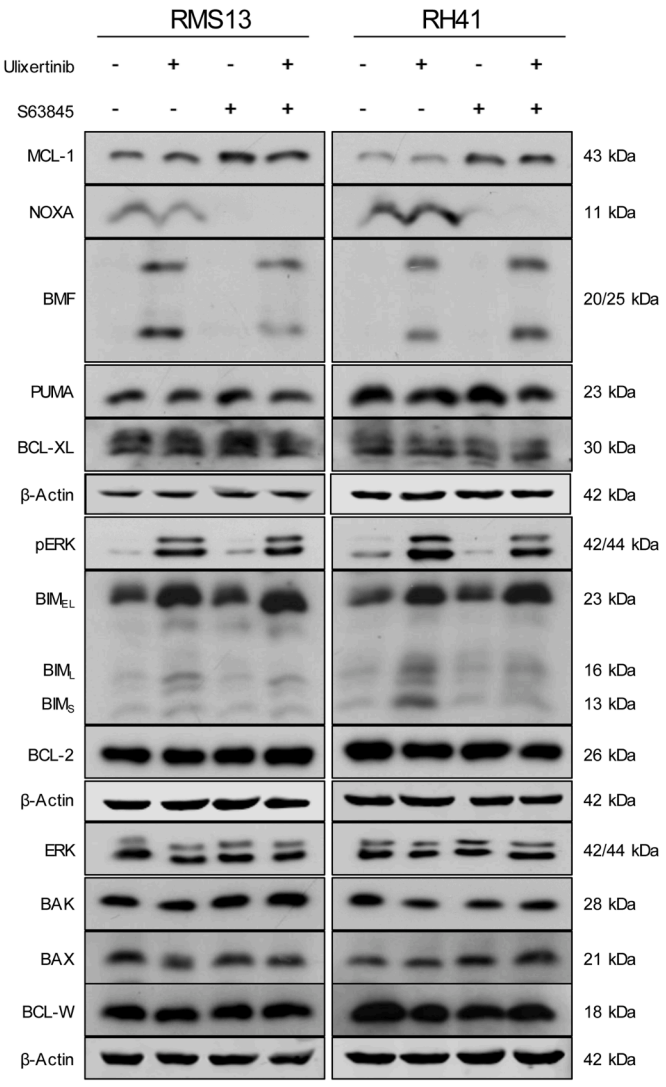

Fig. 5. Ulixertinib/S63845 co-treatment changes the expression of pro- and anti-apoptotic proteins
RMS13 and RH41 cells were treated with 6 μM Ulixertinib and/or 1 μM S63845 (RMS13) and 2 μM Ulixertinib and/or 0.1 μM S63845 (RH41) for 3 h. Whole-cell lysates were analyzed for indicated proteins using Western blotting. β-actin was used as loading control. Quantitative densitometric values relative to β-actin levels are shown in Suppl. Fig. 5. Representative blots of two independent experiments are shown.

tumors compared to single treatment (Fig. 3E, Suppl. Fig. 2E).

Taken together, our experiments showed that combined inhibition of ERK1/2 and MCL-1 leads to rapid induction of caspase-dependent apoptotic cell death in RMS *in vitro* and *in vivo*.

BAK/BAX are required for Ulixertinib/S63845-induced apoptosis

The multi-domain BAK and BAX proteins are key apoptotic effectors that precede caspase activation. To investigate whether BAK and BAX are required for Ulixertinib/S63845-induced apoptosis, we silenced these proteins using siRNA against BAK or BAX. The efficiency of knockdown was confirmed by Western blotting (Fig. 4A, C). BAK knockdown cells showed a significant reduction in apoptosis in response to Ulixertinib/S63845 combination treatment in RMS13 and RH41 cell lines (Fig. 4B), whereas cells with reduced BAX expression exhibited more moderate effects (Fig. 4D). These results indicate that combined inhibition of ERK1/2 and MCL-1 triggers canonical BAK/BAX-dependent intrinsic apoptosis in RMS cells.

Ulixertinib/S63845 co-treatment changes the expression of pro- and anti-apoptotic proteins

Next, we investigated how combined inhibition of ERK1/2 and MCL-1 changes the expression of the BCL-2 family proteins, the upstream regulators of BAK and BAX. Expression levels of phosphorylated ERK1/2 and total MCL-1 were used as markers of Ulixertinib and S63845 compound activity, respectively. Unexpectedly, inhibition of ERK1/2 signaling with Ulixertinib upregulated phosphorylation of ERK1/2 (Fig. 5). However, ERK1/2 downstream targets were suppressed upon Ulixertinib treatment as demonstrated by the reduction in DUSP6 (Dual Specificity Phosphatase 6) levels and dephosphorylation of RSK (the p90 ribosomal s6 kinase), indicating on-target activity of the drug (Suppl. Fig. 3). Thus, although Ulixertinib increases levels of phosphorylated ERK, it was shown that treatment with Ulixertinib strongly sustained inhibition of ERK1/2 signaling as evidenced by pronounced suppression of ERK1/2 downstream events, including phosphorylation of RSK and DUSP6, which is consistent with other reports [29,30]. These observed events indicate on-target effects of Ulixertinib on ERK1/2 inhibition [14]. Similar effects on pERK upregulation were shown for another ERK inhibitor, *i.e.* GDC-0994 [31]. This paradoxical effect on pERK may serve as a biomarker of Ulixertinib activity and be attributed to the mechanisms of action of many ERK inhibitors [14].

As expected, S63845 increased expression levels of MCL-1 (Fig. 5), reflecting its stabilization as described previously [32]. To confirm this hypothesis, we performed cycloheximide (CHX) chase experiments. Once *de novo* protein synthesis was suppressed with the translation inhibitor CHX, the stability of MCL-1 was increased in the presence of S63845 (Suppl. Fig. 4B, C). These data imply that S63845 stabilized MCL-1 and prevented its degradation. Treatment with S63845 also resulted in the reduction of NOXA expression (Fig. 5). We demonstrated that Ulixertinib alone or in combination with S63845 induced expression of the pro-apoptotic proteins BIM and BMF, while the combination had a modest effect on the expression levels of other pro- and anti-apoptotic proteins (Fig. 5). To test whether the S63845 treatment allows displacement of MCL-1 from upregulated BIM and BMF, we immunoprecipitated MCL-1 and analyzed its binding to BIM and BMF. Interestingly, we demonstrated that treatment with S63845 alone and in combination with Ulixertinib strikingly reduced BMF and BIM binding to MCL-1 (Suppl. Fig. 4A), resulting in accumulation of unbound BIM and BMF and facilitating their interaction with other anti-apoptotic BCL-2 proteins.

Therefore, these results suggest that BMF and BIM may be crucial regulators of Ulixertinib/S63845-induced apoptosis and, together with the neutralization of MCL-1 activity, shift the balance of pro- and anti-apoptotic proteins towards cell death induction.

Activation of BIM and BMF as well as neutralization of MCL-1 are essential for cell death induction upon ERK1/2 inhibition

To investigate whether BMF and BIM are required for Ulixertinib/S63845-induced apoptosis, we performed knockdown of BIM and BMF using three siRNA sequences for each gene. Knockdown efficiency was controlled using Western blot analysis (Fig. 6A, C). Importantly, knockdown of BIM and BMF significantly reduced apoptosis triggered by Ulixertinib/S63845 combination treatment (Fig. 6B, D). These findings demonstrate that activation of BIM and BMF is a key step in the induction of apoptosis following ERK1/2 inhibition.

To confirm the requirement of MCL-1 suppression for cell death induction upon ERK1/2 inhibition, we performed an MCL-1 knockdown and treated cells with Ulixertinib. The efficiency of MCL-1 knockdown was confirmed using Western blotting (Fig. 6E). Indeed, suppression of MCL-1 expression cooperated with Ulixertinib to induce cell death (Fig. 6F). Taken together, these studies highlight that MCL-1 provides a key block in apoptosis induced by ERK1/2 inhibitors, and that its neutralization either by pharmacological inhibitors or by genetic

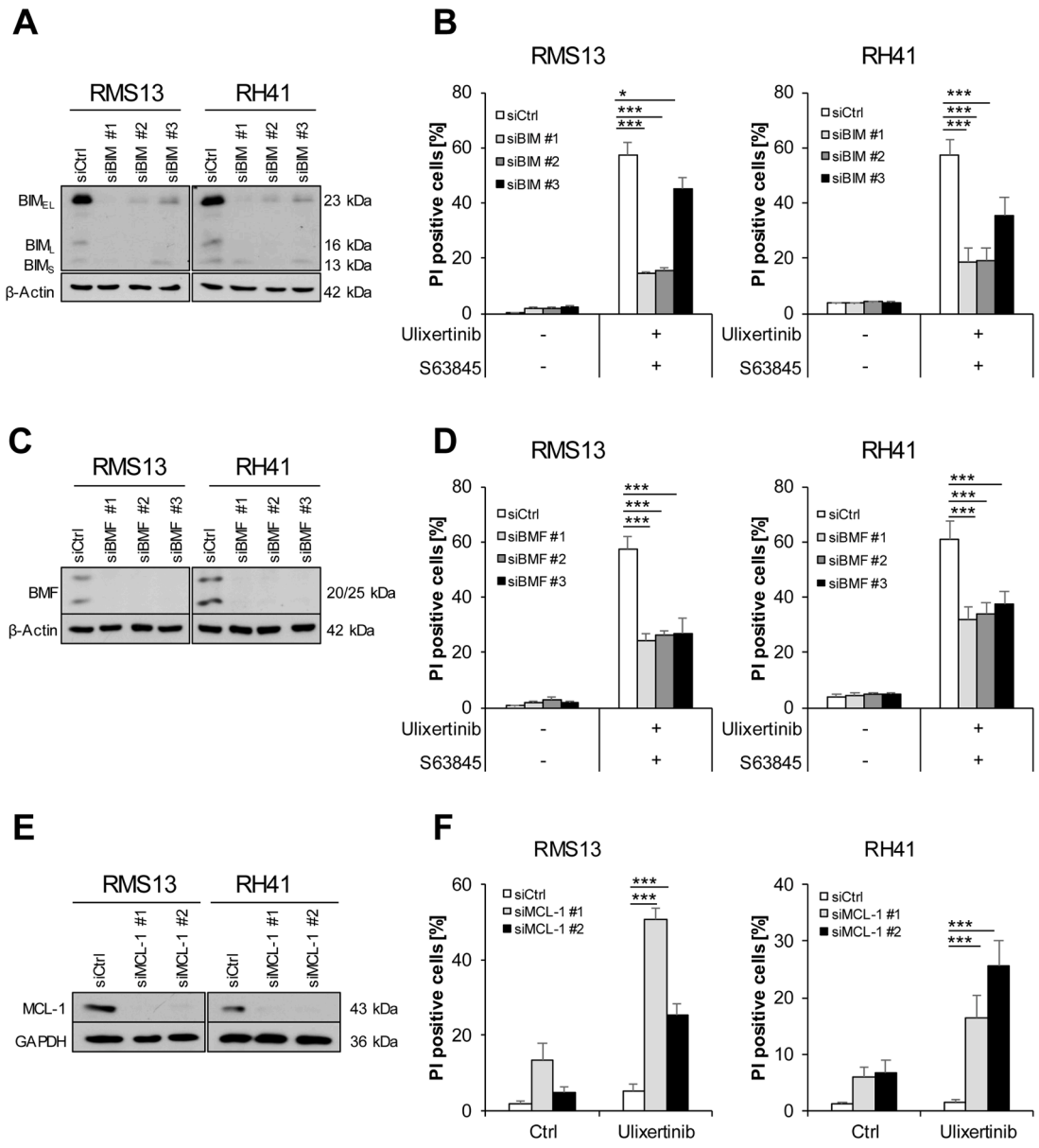

Fig. 6. BIM, BMF and MCL-1 are key players in cell death induction upon Ulixertinib/S63845 co-treatment
RMS13 and RH41 cells were transiently transfected with non-silencing siRNA (siCtrl) or three distinct siRNA sequences targeting BIM (siBIM #1, siBIM #2, siBIM #3) or BMF (siBMF #1, siBMF #2, siBMF #3) and treated with 6 μM Ulixertinib and/or 1 μM S63845 (RMS13) and 2 μM Ulixertinib and/or 0.1 μM S63845 (RH41). Expression of BIM and BMF was assessed by Western blotting after 48 h. β-actin was used as loading control. Representative blots of two independent experiments are shown (A, C). Cell death was measured after 72 h by fluorescence microscopy analysis of PI uptake using Hoechst 33342 and PI co-staining (B, D). RMS13 and RH41 cells were transiently transfected with non-silencing siRNA (siCtrl) or two distinct siRNA sequences targeting MCL-1 (siMCL-1 #1, siMCL-1 #2) and treated as in B, D above. Expression of MCL-1 was assessed by Western blotting after 48 h. GAPDH was used as a loading control. Representative blots of two independent experiments are shown (E). Cell death was measured after 72 h using PI andHoechst 33342 co-staining (F). Mean and SD (error bars) of three independent experiments performed in triplicates are shown, *, $P < 0.05$; ***, $P < 0.001$.

silencing is required for apoptosis to occur.

BCL-2 overexpression rescues RMS13 and RH41 cells from Ulixertinib/S63845-induced apoptosis

To further investigate the molecular mechanisms underlying Ulixertinib/S63845-induced cell death, we generated RMS13 and RH41 cells ectopically expressing pro-survival BCL-2 protein. Overexpression of BCL-2 was confirmed by Western blot analysis (Fig. 7A). Importantly, BCL-2 overexpression significantly reduced Ulixertinib/S63845-triggered cell death in RMS13 and RH41 cells (Fig. 7B). These results demonstrate that BCL-2 overexpression prevents cell death induction upon the combination treatment, highlighting the role of the intrinsic mitochondrial pathway.

Discussion

ERK1/2 signaling is often hyperactive in RMS, including those with activated RAS mutations and FP-RMS, however, MEK1/2 inhibitors have shown limited efficiency as monotherapy in RMS cells, as well as in other cancer types [10]. Responses to MEK1/2 inhibitors in preclinical and clinical studies are transient due to the activation of resistance mechanisms that re-activate the ERK1/2 kinase. Additionally, adaptive responses of cells to MEK1/2 inhibition via neutralization of apoptotic

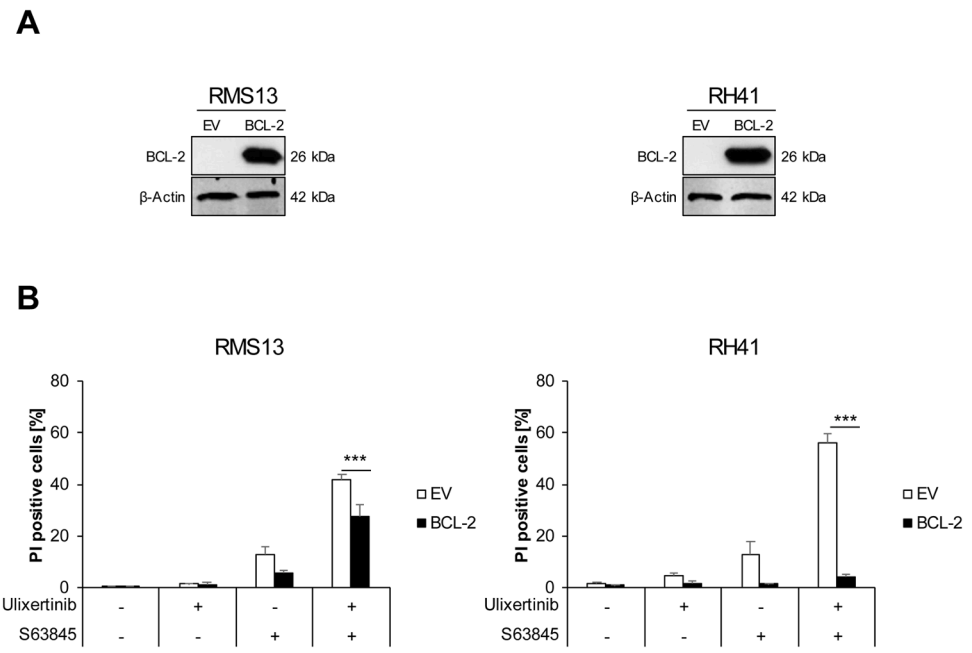

Fig. 7. BCL-2 overexpression rescues RMS13 and RH41 cells from Ulixertinib/S63845-induced apoptosis

RMS13 and RH41 cells were transfected with EV or murine BCL-2 construct (BCL-2). BCL-2 overexpression was confirmed by Western blotting. β-actin was used as loading control. Representative blots of two independent experiments are shown (A). Transfected cells were treated with 6 μM Ulixertinib and/or 1 μM S63845 (RMS13) and 2 μM Ulixertinib and/or 0.1 μM S63845 (RH41) for 72 h. Cell death was measured after 72 h by fluorescent microscopy analysis of PI uptake using Hoechst 33342 and PI co-staining (B). Mean and SD (error bars) of three independent experiments performed in triplicates are shown, ***, $P < 0.001$.

signaling by pro-survival BCL-2 family proteins also contribute to the limited efficiency of RAS/MEK/ERK signaling inhibition as monotherapy. In RMS, MCL-1 is often overexpressed [21] and represents a significant barrier that prevents apoptosis following the inhibition of RAS/MEK/ERK signaling.

Therefore, we wanted to investigate the impact of combined exposure of RMS cells to selective ERK1/2 inhibitors and MCL-1 inhibitors. Here, we identified a synergism between ERK1/2 inhibitors (Ulixertinib and SCH772984) and MCL-1 inhibitor (S63845) to induce cell death in RMS cells, whereas monotherapy with each compound showed no effect or minimal response. The highly synergistic effect of Ulixertinib and S63845 on cell death was underlined by calculation of Bliss score. Furthermore, the potency of this combination treatment is supported by data showing that colony formation ability is significantly suppressed upon Ulixertinib/S63845 co-treatment. These results are of particular interest, since the RTK/RAS/MEK/ERK axis is commonly dysregulated in RMS [6]. In the present study, we demonstrated that co-inhibition of ERK1/2 and MCL-1 effectively triggers cell death in both FP-RMS and FN-RMS, showing a more general therapeutic potential that is restricted not only to FN-RMS driven by RAS mutations. In contrast to RMS cells, the combination of Ulixertinib and S63845 failed to induce cell death in non-malignant cells, indicating some cancer selectivity of this combination. The concentrations tested in this study are not toxic to non-malignant cell lines or human PBMCs, emphasizing the possibility of a therapeutic window in which RMS cells are undergoing apoptosis while normal cells are less affected. This may be due to the observation that predominantly higher levels of MCL-1 expression were found in RMS cells compared to normal cells [24,33]. Beside, several studies have shown high expression in RMS samples of different receptor tyrosine kinases that might activate ERK1/2 signaling [6,34,35].

Mechanistically, co-treatment with Ulixertinib and S63845 resulted in caspase-dependent apoptosis as evidenced by rapid caspase-3/7 activation, accumulation of fragmented DNA, increase in Annexin V-positive cells, cleavage of PARP, procaspase-3 and procaspase-9, and an almost complete rescue of cell death upon addition of pan-caspase inhibitor zVAD.fmk. We demonstrated that Ulixertinib-mediated upregulation of BIM and BMF in combination with MCL-1 inhibition by S63845 shifts the balance of BCL-2 proteins towards a pro-apoptotic state and that this is an important molecular event that contributes to synergistic apoptosis induction by Ulixertinib/S63845 co-treatment. This Ulixertinib/S63845-induced apoptosis required upregulated BIM and BMF expression, since genetic silencing of these proteins significantly rescued cell death. Despite strong upregulation of pro-apoptotic proteins following Ulixertinib treatment, inhibition of RAS/MEK/ERK signaling alone is not sufficient to induce cell death in RMS, which is in line with our previous studies [20,36]. Here, we demonstrated that inhibition of MCL-1 is required to induce apoptosis when ERK1/2 signaling is suppressed, as supported by pharmacological and genetic approaches, showing that specific inhibition or knockdown of MCL-1 cooperate with Ulixertinib to trigger cell death. In line with previous studies, the MCL-1 engagement by S63845 single treatment or the combination was demonstrated by increased protein levels of MCL-1 [32]. Increased MCL-1 expression upon addition of S63845 might be explained by its stabilization due to displacement of MULE (MCL-1 ubiquitin ligase E3) from BH3 domain of MCL-1, reducing proteasome degradation of MCL-1 [37]. Furthermore, we showed that the stability of MCL-1 was increased by the presence of S63845 when protein translation was inhibited with CHX. It has been reported that in non-small-cell lung carcinoma cell lines with mutated KRAS, high expression levels of MCL-1 protein neutralize BIM that is upregulated upon MEK inhibition [22]. Also, we demonstrated that the addition of S63845 displaces MCL-1 from BIM and BMF which are strongly upregulated upon Ulixertinib treatment, highlighting the potency of the combination. These changes in pro- and anti-apoptotic BCL-2 proteins result in activation of multidomain pro-apoptotic BAK and BAX. Our data also emphasize the crucial role of the intrinsic mitochondrial pathway in Ulixertinib/S63845-induced apoptosis, as BAK and BAX silencing or overexpression of the anti-apoptotic protein BCL-2 prevented cell death.

Therapeutic options of co-targeting pro-survival pathways and regulators of apoptosis have a potential to increase treatment efficiency and overcome treatment resistance and treatment-associated toxicities [38]. The targeting of ERK1/2 signaling in RMS is of clinical relevance, as aberrant activation of this pathway has frequently been observed in the majority of patients [6]. Ulixertinib is the first ERK1/2 inhibitor that is well-tolerated in patients and has demonstrated clinical response in solid tumors with dysregulated RAS/MEK/ERK signaling [13]. MCL-1 inhibitors have not yet reached the stage of clinical application, however, S63845 showed a favorable safety window in mouse models [39]. Importantly, our study revealed that Ulixertinib/S63845 combination demonstrated antitumor effects in the CAM *in vivo* model as reflected by

increased caspase-3 activity. Therefore, combining Ulixertinib and S63845 might have clinical potential and promote clinical translation of these compounds.

In conclusion, in this study we demonstrated a synergistic effect of combined ERK1/2 and MCL-1 inhibition *in vitro* and *in vivo*. Interestingly, the combination of ERK1/2 inhibitor and MCL-1 inhibitor was effective in RMS cell lines regardless of PAX3/7-FOXO1 fusion or RAS mutational status, suggesting that this combination could be beneficial for a wide range of RMS patients. These findings provide a basis for novel therapeutic options for RMS patients with hyperactive ERK1/2 signaling.

CRediT authorship contribution statement

Marius Winkler: Investigation, Formal analysis, Writing – original draft, Writing – review & editing. **Juliane Friedrich:** Methodology, Writing – original draft, Writing – review & editing. **Cathinka Boedicker:** Writing – review & editing. **Nadezda Dolgikh:** Investigation, Formal analysis, Conceptualization, Writing – original draft, Writing – review & editing.

Declaration of Competing Interest

None to declare.

Acknowledgments

We thank C. Hugenberg for expert secretarial assistance and D. Brücher for expert technical assistance. This study has been supported by the Mildred-Scheel-Nachwuchszentrum Frankfurt (70113301), funded by the Deutsche Krebshilfe e.V. (to M.W.).

Supplementary materials

Supplementary material associated with this article can be found, in the online version, at doi:10.1016/j.tranon.2021.101313.

References

[1] M.A. Arnold, F.G. Barr, Molecular diagnostics in the management of rhabdomyosarcoma, Expert Rev. Mol. Diagn. 17 (2017) 189–194.
[2] A. Pal, H.Y. Chiu, R. Taneja, Genetics, epigenetics and redox homeostasis in rhabdomyosarcoma: emerging targets and therapeutics, Redox. Biol. 25 (2019), 101124.
[3] J.C. Breneman, E. Lyden, A.S. Pappo, M.P. Link, J.R. Anderson, D.M. Parham, S. J. Qualman, M.D. Wharam, S.S. Donaldson, H.M. Maurer, W.H. Meyer, K.S. Baker, C.N. Paidas, W.M. Crist, Prognostic factors and clinical outcomes in children and adolescents with metastatic rhabdomyosarcoma–a report from the intergroup rhabdomyosarcoma study IV, J. Clin. Oncol. 21 (2003) 78–84.
[4] R. Garcia-Gomez, X.R. Bustelo, P. Crespo, Protein-protein interactions: emerging oncotargets in the RAS-ERK pathway, Trends Cancer 4 (2018) 616–633.
[5] R. Roskoski, Targeting ERK1/2 protein-serine/threonine kinases in human cancers, Pharmacol. Res. 142 (2019) 151–168.
[6] J.F. Shern, L. Chen, J. Chmielecki, J.S. Wei, R. Patidar, M. Rosenberg, L. Ambrogio, D. Auclair, J. Wang, Y.K. Song, C. Tolman, L. Hurd, H. Liao, S. Zhang, D. Bogen, A. S. Brohl, S. Sindiri, D. Catchpoole, T. Badgett, G. Getz, J. Mora, J.R. Anderson, S. X. Skapek, F.G. Barr, M. Meyerson, D.S. Hawkins, J. Khan, Comprehensive genomic analysis of rhabdomyosarcoma reveals a landscape of alterations affecting a common genetic axis in fusion-positive and fusion-negative tumors, Cancer Discov. 4 (2014) 216–231.
[7] B. Zhu, J.K. Davie, New insights into signalling-pathway alterations in rhabdomyosarcoma, Br. J. Cancer 112 (2015) 227–231.
[8] U. Degirmenci, M. Wang, J. Hu, Targeting aberrant RAS/RAF/MEK/ERK signaling for cancer therapy, Cells 9 (2020) 1–34.
[9] M. Holderfield, M.M. Deuker, F. McCormick, M. McMahon, Targeting RAF kinases for cancer therapy: bRAF-mutated melanoma and beyond, Nat. Rev. Cancer 14 (2014) 455–467.
[10] C.J. Caunt, M.J. Sale, P.D. Smith, S.J. Cook, MEK1 and MEK2 inhibitors and cancer therapy: the long and winding road, Nat. Rev. Cancer 15 (2015) 577–592.
[11] M.S. Carlino, J.R. Todd, K. Gowrishankar, B. Mijatov, G.M. Pupo, C. Fung, S. Snoyman, P. Hersey, G.V. Long, R.F. Kefford, H. Rizos, Differential activity of MEK and ERK inhibitors in BRAF inhibitor resistant melanoma, Mol. Oncol. 8 (2014) 544–554.
[12] F. Liu, X. Yang, M. Geng, M. Huang, E.R.K. Targeting, Achilles an, Heel of the MAPK pathway, in cancer therapy, Acta Pharm. Sin. B 8 (2018) 552–562.
[13] R.J. Sullivan, J.R. Infante, F. Janku, D.J.L. Wong, J.A. Sosman, V. Keedy, M. R. Patel, G.I. Shapiro, J.W. Mier, A.W. Tolcher, A. Wang-Gillam, M. Sznol, K. Flaherty, E. Buchbinder, R.D. Carvajal, A.M. Varghese, M.E. Lacouture, A. Ribas, S.P. Patel, G.A. DeCrescenzo, C.M. Emery, A.L. Groover, S. Saha, M. Varterasian, D. J. Welsch, D.M. Hyman, B.T. Li, First-in-class ERK1/2 inhibitor ulixertinib (BVD-523) in patients with MAPK mutant advanced solid tumors: results of a phase I dose-escalation and expansion study, Cancer Discov. 8 (2018) 184–195.
[14] U.A. Germann, B.F. Furey, W. Markland, R.R. Hoover, A.M. Aronov, J.J. Roix, M. Hale, D.M. Boucher, D.A. Sorrell, G. Martinez-Botella, M. Fitzgibbon, P. Shapiro, M.J. Wick, R. Samadani, K. Meshaw, A. Groover, G. DeCrescenzo, M. Namchuk, C.M. Emery, S. Saha, D.J. Welsch, Targeting the MAPK signaling pathway in cancer: promising preclinical activity with the novel selective ERK1/2 inhibitor BVD-523 (Ulixertinib), Mol. Cancer Ther. 16 (2017) 2351–2363.
[15] B.A. Carneiro, W.S. El-Deiry, Targeting apoptosis in cancer therapy, Nat. Rev. Clin. Oncol. 17 (2020) 395–417.
[16] S. Fulda, L. Galluzzi, G. Kroemer, Targeting mitochondria for cancer therapy, Nat. Rev. Drug Discov. 9 (2010) 447–464.
[17] R.C. Taylor, S.P. Cullen, S.J. Martin, Apoptosis: controlled demolition at the cellular level, Nat. Rev. Mol. Cell Biol. 9 (2008) 231–241.
[18] R. Singh, A. Letai, K. Sarosiek, Regulation of apoptosis in health and disease: the balancing act of BCL-2 family proteins, Nat. Rev. Mol. Cell Biol. 20 (2019) 175–193.
[19] A. Kotschy, Z. Szlavik, J. Murray, J. Davidson, A.L. Maragno, G. Le Toumelin-Braizat, M. Chanrion, G.L. Kelly, J.N. Gong, D.M. Moujalled, A. Bruno, M. Csekei, A. Paczal, Z.B. Szabo, S. Sipos, G. Radics, A. Proszenyak, B. Balint, L. Ondi, G. Blasko, A. Robertson, A. Surgenor, P. Dokurno, I. Chen, N. Matassova, J. Smith, C. Pedder, C. Graham, A. Studeny, G. Lysiak-Auvity, A.M. Girard, F. Grave, D. Segal, C.D. Riffkin, G. Pomilio, L.C. Galbraith, B.J. Aubrey, M.S. Brennan, M. J. Herold, C. Chang, G. Guasconi, N. Cauquil, F. Melchiore, N. Guigal-Stephan, B. Lockhart, F. Colland, J.A. Hickman, A.W. Roberts, D.C. Huang, A.H. Wei, A. Strasser, G. Lessene, O. Geneste, The MCL1 inhibitor S63845 is tolerable and effective in diverse cancer models, Nature 538 (2016) 477–482.
[20] N. Dolgikh, M. Hugle, M. Vogler, S. Fulda, NRAS-mutated rhabdomyosarcoma cells are vulnerable to mitochondrial apoptosis induced by coinhibition of MEK and PI3Kalpha, Cancer Res. 78 (2018) 2000–2013.
[21] L. Pazzaglia, A. Chiechi, A. Conti, G. Gamberi, G. Magagnoli, C. Novello, L. Morandi, P. Picci, M. Mercuri, M.S. Benassi, Genetic and molecular alterations in rhabdomyosarcoma: mRNA overexpression of MCL1 and MAP2K4 genes, Histol. Histopathol. 24 (2009) 61–67.
[22] V. Nangia, F.M. Siddiqui, S. Caenepeel, D. Timonina, S.J. Bilton, N. Phan, M. Gomez-Caraballo, H.L. Archibald, C. Li, C. Fraser, D. Rigas, K. Vajda, L.A. Ferris, M. Lanuti, C.D. Wright, K.A. Raskin, D.P. Cahill, J.H. Shin, C. Keyes, L.V. Sequist, Z. Piotrowska, A.F. Farago, C.G. Azzoli, J.F. Gainor, K.A. Sarosiek, S.P. Brown, A. Coxon, C.H. Benes, P.E. Hughes, A.N. Hata, Exploiting MCL1 dependency with combination MEK + MCL1 inhibitors leads to induction of apoptosis and tumor regression in KRAS-mutant non-small cell lung cancer, Cancer Discov. 8 (2018) 1598–1613.
[23] S. Fulda, H. Sieverts, C. Friesen, I. Herr, K.M. Debatin, The CD95 (APO-1/Fas) system mediates drug-induced apoptosis in neuroblastoma cells, Cancer Res. 57 (1997) 3823–3829.
[24] S. Kehr, T. Haydn, A. Bierbrauer, B. Irmer, M. Vogler, S. Fulda, Targeting BCL-2 proteins in pediatric cancer: dual inhibition of BCL-XL and MCL-1 leads to rapid induction of intrinsic apoptosis, Cancer Lett. 482 (2020) 19–32.
[25] M. Hugle, K. Belz, S. Fulda, Identification of synthetic lethality of PLK1 inhibition and microtubule-destabilizing drugs, Cell Death Differ. 22 (2015) 1946–1956.
[26] A. Ianevski, L. He, T. Aittokallio, J. Tang, SynergyFinder: a web application for analyzing drug combination dose-response matrix data, Bioinformatics 33 (2017) 2413–2415.
[27] T.C. Chou, Drug combination studies and their synergy quantification using the Chou-Talalay method, Cancer Res. 70 (2010) 440–446.
[28] M. Vogler, H. Walczak, D. Stadel, T.L. Haas, F. Genze, M. Jovanovic, J. E. Gschwend, T. Simmet, K.M. Debatin, S. Fulda, Targeting XIAP bypasses Bcl-2-mediated resistance to TRAIL and cooperates with TRAIL to suppress pancreatic cancer growth *in vitro* and *in vivo*, Cancer Res. 68 (2008) 7956–7965.
[29] H. Jiang, M. Xu, L. Li, P. Grierson, P. Dodhiawala, M. Highkin, D. Zhang, Q. Li, A. Wang-Gillam, K.H. Lim, Concurrent HER or PI3K inhibition potentiates the antitumor effect of the ERK inhibitor ulixertinib in preclinical pancreatic cancer models, Mol. Cancer Ther. 17 (2018) 2144–2155.
[30] I. Valencia-Sama, Y. Ladumor, L. Kee, T. Adderley, G. Christopher, C.M. Robinson, Y. Kano, M. Ohh, M.S. Irwin, NRAS status determines sensitivity to SHP2 inhibitor combination therapies targeting the RAS-MAPK pathway in neuroblastoma, Cancer Res. 80 (2020) 3413–3423.
[31] M. Merchant, J. Moffat, G. Schaefer, J. Chan, X. Wang, C. Orr, J. Cheng, T. Hunsaker, L. Shao, S.J. Wang, M.C. Wagle, E. Lin, P.M. Haverty, S. Shahidi-Latham, H. Ngu, M. Solon, J. Eastham-Anderson, H. Koeppen, S.A. Huang, J. Schwarz, M. Belvin, D. Kirouac, M.R. Junttila, Combined MEK and ERK inhibition overcomes therapy-mediated pathway reactivation in RAS mutant tumors, PLoS ONE 12 (2017), e0185862.
[32] Z. Li, S. He, A.T. Look, The MCL1-specific inhibitor S63845 acts synergistically with venetoclax/ABT-199 to induce apoptosis in T-cell acute lymphoblastic leukemia cells, Leukemia 33 (2019) 262–266.
[33] A.D. Marshall, F. Picchione, R.I. Geltink, G.C. Grosveld, PAX3-FOXO1 induces up-regulation of Noxa sensitizing alveolar rhabdomyosarcoma cells to apoptosis, Neoplasia 15 (2013) 738–748.

[34] P.M. Armistead, J. Salganick, J.S. Roh, D.M. Steinert, S. Patel, M. Munsell, A.K. El-Naggar, R.S. Benjamin, W. Zhang, J.C. Trent, Expression of receptor tyrosine kinases and apoptotic molecules in rhabdomyosarcoma: correlation with overall survival in 105 patients, Cancer 110 (2007) 2293–2303.
[35] L. Cao, Y. Yu, I. Darko, D. Currier, L.H. Mayeenuddin, X. Wan, C. Khanna, L. J. Helman, Addiction to elevated insulin-like growth factor I receptor and initial modulation of the AKT pathway define the responsiveness of rhabdomyosarcoma to the targeting antibody, Cancer Res. 68 (2008) 8039–8048.
[36] M.K. Guenther, U. Graab, S. Fulda, Synthetic lethal interaction between PI3K/Akt/mTOR and Ras/MEK/ERK pathway inhibition in rhabdomyosarcoma, Cancer Lett. 337 (2013) 200–209.
[37] Q. Zhong, W. Gao, F. Du, X. Wang, Mule/ARF-BP1, a BH3-only E3 ubiquitin ligase, catalyzes the polyubiquitination of Mcl-1 and regulates apoptosis, Cell 121 (2005) 1085–1095.
[38] M.S. Cragg, C. Harris, A. Strasser, C.L. Scott, Unleashing the power of inhibitors of oncogenic kinases through BH3 mimetics, Nat. Rev. Cancer 9 (2009) 321–326.
[39] M.S. Brennan, C. Chang, L. Tai, G. Lessene, A. Strasser, G. Dewson, G.L. Kelly, M. J. Herold, Humanized Mcl-1 mice enable accurate preclinical evaluation of MCL-1 inhibitors destined for clinical use, Blood 132 (2018) 1573–1583.